

Erosion regulation as a function of human disturbances to vegetation cover: a conceptual model

Veerle Vanacker · Nicolas Bellin ·
Armando Molina · Peter W. Kubik

Received: 1 April 2013 / Accepted: 21 October 2013 / Published online: 8 November 2013
© Springer Science+Business Media Dordrecht 2013

Abstract Human-induced land cover changes are causing important effects on the ecological services rendered by mountain ecosystems, and the number of case-studies of the impact of humans on soil erosion and sediment yield has mounted rapidly. In this paper, we present a conceptual model that allows evaluating overall changes in erosion regulation after human disturbances. The basic idea behind this model is that soil erosion mechanisms are independent of human impact, but that the frequency–magnitude distributions of erosion rates change as a response to human disturbances. Pre-disturbance (or natural) erosion rates are derived from in situ produced ^{10}Be concentrations in river sediment, while post-disturbance (or modern) erosion rates are derived from sedimentation rates in small catchments. In its simplicity, the model uses vegetation cover change as a proxy of human disturbance. The erosion regulation model is here

applied in two mountainous regions with different vegetation dynamics, climatic and geological settings: the Austro Ecuatoriano, and the Spanish Betic Cordillera. Natural erosion benchmarks are necessary to assess human-induced changes in erosion rates. While the Spanish Betic Cordillera is commonly characterized as a degraded landscape, there is no significant difference between modern catchment-wide erosion and long-term denudation rates. The opposite is true for the Austro Ecuatoriano where the share of natural erosion in the total modern erosion rate is minimal for most disturbed sites. When pooling pre- and post-disturbance erosion data from both regions, the data suggest that the human acceleration of erosion is related to vegetation disturbances. The empirical regression model predicts human acceleration of erosion, here defined as the ratio of post-disturbance to pre-disturbance (or natural benchmark) erosion rate, as an exponential function of vegetation disturbance. This suggests that the sensitivity to human-accelerated erosion would be ecosystem dependent, and related to the potential vegetation cover disturbances as a result of human impact. It may therefore be expected that the potential for erosion regulation is larger in well-vegetated ecosystem where strong differences may exist in vegetation cover between human disturbed and undisturbed or restored sites.

V. Vanacker (✉) · N. Bellin
Earth and Life Institute, Georges Lemaître Centre for
Earth and Climate Research, Université Catholique de
Louvain, Louvain-la-Neuve, Belgium
e-mail: veerle.vanacker@uclouvain.be

A. Molina
Soil Science of Tropical and Subtropical Ecosystems,
Büsgen Institute, Georg-August-Universität Göttingen,
Göttingen, Germany

P. W. Kubik
Laboratory of Ion Beam Physics, ETH Zürich,
8093 Zurich, Switzerland

Keywords Erosion regulation potential ·
Human acceleration of erosion · Mountain
regions · Land cover change · Human impact

Introduction

Mountain regions present unique challenges and opportunities to land use change research (Garcia-Ruiz et al. 1996; MacDonald et al. 2000; Schröter et al. 2005). Very few, if any, mountain ecosystems remain unaffected by human impact (Pauchard et al. 2009). The landscape pattern and structure that are currently perceived in mountain reserves and parks are often strongly influenced by past human occupation (Huber et al. 2005). For centuries, mountain regions have been the subject of colonization to create space for agriculture and grazing. Traditionally, human population in mountain regions is concentrated in the lower valleys because of the milder climate and more favorable conditions for agricultural development. During periods of political instability or increasing land pressure, migration often occurs toward higher and more remote mountain regions. These steep and remote ecosystems are particularly sensitive to accelerated soil erosion, slope movements, and rapid loss of habitat and genetic diversity (Jandl et al. 2009). Although traditional mountain agriculture is being abandoned in many mountain regions worldwide (MacDonald et al. 2000; Lambin and Meyfroidt 2010), it continues to expand in developing countries. This is mainly the case in marginal regions where subsistence agriculture remains a major contributor of the local economy (Jha and Bawa 2006).

The Millennium Ecosystem Assessment recognizes the central role that mountain ecosystems play in supporting human well-being. Although mountain regions constitute only one-fifth of the terrestrial surface, more than half of the global human population depends directly or indirectly on mountain resources (Millennium Ecosystem Assessment 2005). Mountain rivers play a vital role in regulating the freshwater supply to the growing populations in the mountains and adjacent lowlands (Viviroli et al. 2007). As such, they support key environmental services such as regulation of water flow and quality for domestic use, agriculture and industry; biodiversity conservation and hydropower generation.

Because of the fragility of mountain ecosystems, human-induced land use changes are expected to have important implications for the future supply of environmental services (Foley et al. 2005; FAO 2011). The number of case studies that illustrate the impact of changing land use systems in mountain areas on the

quality and/or quantity of freshwater resources has mounted rapidly (Löffler et al. 2011). Although these case studies are very valuable, they are only representative for a narrow range of environmental conditions given that mountain environments typically display steep environmental gradients over short distances. There are currently no consistent data on the overall importance of humans as modifiers of freshwater resources for entire mountain ranges.

Besides, a modelling framework that is specifically adapted to mountain environments is currently lacking. Most studies make use of general river basin models (such as RUSLE, Renard et al. 1998; or SWAT, Arnold et al. 2012) that were originally parameterized and calibrated for temperate, low relief landscapes (e.g. Stehr et al. 2010). Transposing these modelling concepts directly to steep environments with shallow and stony soils often leads to unrealistic model predictions, as model input parameters are rarely calibrated for the range of environmental conditions found in mountain regions (Fohrer et al. 2005). This is particularly the case for the empirical soil erosion models (USLE/RUSLE) that continue to play an important role in tools for modelling freshwater ecosystem services such as in VEST or ARIES (Vigerstol and Aukema 2011).

Here, we present a conceptual model that evaluates erosion regulation as a function of human disturbances in vegetation cover. Erosion regulation is here defined as the potential reduction in catchment-wide erosion rates resulting from changes in vegetation cover. It is an indicator of the vulnerability of a given ecosystem to human-induced land cover change. The erosion regulation potential is estimated as the ratio of the total specific sediment yield to the natural benchmark denudational mass flux, and is dimensionless. Data on potential erosion regulation are obtained through three independent assessment tools: (1) in situ produced cosmogenic radionuclides to establish natural benchmark denudational mass fluxes, (2) reservoir sedimentation measurements to establish average specific sediment yields, and (3) remote sensing to reconstruct vegetation cover change through time. All erosion measures are taken at the spatial scale of small to medium sized catchments (0.01 up to 276 km²). As the sampling sites are dominated by erosional processes, the sediment fluxes can be converted to catchment-wide erosion rates. The empirical erosion regulation model is calibrated for two mountainous regions located in the semi-arid Internal Zone of the Betic

Cordillera in the West-Mediterranean (Spain) and the Austro Ecuatoriano (Southern Ecuadorian Andes).

Theoretical background

The intrinsic physical mechanisms of soil erosion by water are likely to be independent of human disturbances, as the fundamental mechanistic processes of soil production, transport, and deposition have not changed since the Anthropocene. There is no unique erosion mechanism that is solely linked to human activities. Instead, human activities have altered the magnitude and frequency of erosion events (Corenblit and Steiger 2009; Reinhardt et al. 2010). Figure 1 illustrates this concept that is based on the seminal paper by Dietrich and Perron (2006) on the topographic signature of life. If we would compare erosion rates between hypothetical prehistoric and modern landscapes, this conceptual model suggests that the frequency distributions of erosion rates would be different. Landscapes with strong human impact are then predicted to have higher frequencies of high magnitude erosion events.

The most apparent human modification to mountain ecosystems is the disturbance of native vegetation communities. Vegetation strongly controls the frequency and magnitude of erosion events (Thornes 1990; Viles et al. 2008). Vegetation communities

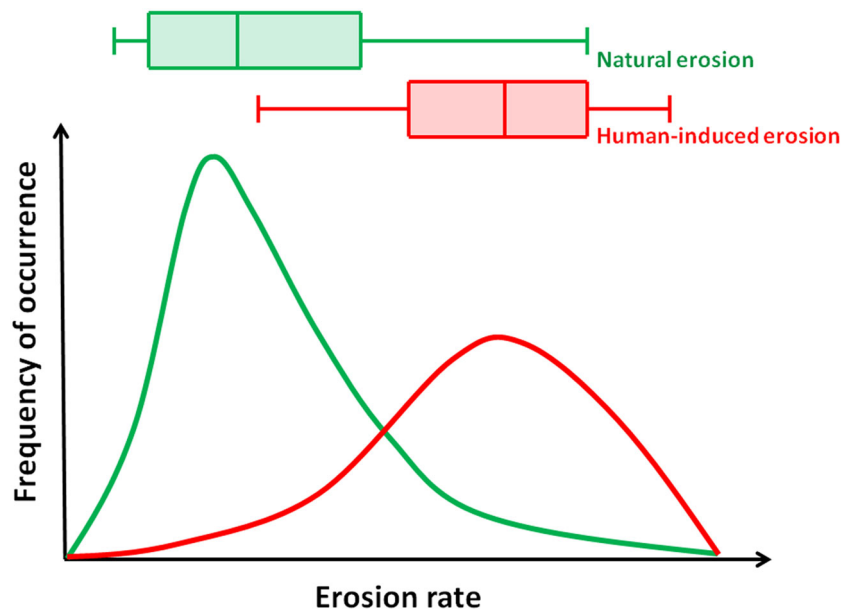
directly affect soil physical and chemical properties through modifications in (1) net rainfall and raindrop energy by canopy interception, (2) soil water content by plant transpiration, (3) surface roughness and (4) soil cohesion by the root system (Gyssels et al. 2005). In this study, we hypothesise that the shift in frequency distributions of erosion rates is dependent on the degree of human disturbance of the native vegetation (Fig. 1).

Given the importance of vegetation for sediment regulation, soil erosion models typically include vegetation cover as one of the key model parameters (SWAT, Arnold et al. 2012; USLE, Wischmeier and Smith 1978; RUSLE, Renard et al. 1998). In a review by Gyssels et al. (2005), it is shown that most empirical equations established for splash, rill, and interrill erosion at the plot scale describe the erosion rate (E) as a function of vegetation cover (C , %) by a negative exponential function

$$E = a \times e^{-bc} \quad (1)$$

where a is a constant and function of the local climate, topography and geological setting, and b is a constant indicating the effectiveness of the vegetation in reducing erosion rates. A nonlinear increase in sediment fluxes with decreasing (forest) vegetation cover has also been reported based on catchment-wide erosion rates of small catchments, suggesting the general character of an exponential increase in erosion rates with decreasing vegetation cover (Thornes 1990;

Fig. 1 Hypothetical frequency–magnitude distribution of erosion rates for undisturbed (*green*) and human disturbed (*red*) environments. The boxplots (*on top*) illustrate that human perturbations to mountain ecosystems is expected to lead to a shift in the frequency–magnitude distribution, with more surface area that is subject to high erosion rates. (Color figure online)



Molina et al. 2008). Similarly, field observations show a significant (and nonlinear) decrease in slope stability after root strength decay following vegetation disturbances (Sidle and Ochiai 2006).

Although the empirical erosion models are an interesting starting point, they do not allow one to assess the impact of human disturbances in vegetation cover on erosion regulation potential in mountain rivers. In mountain ecosystems, natural erosion processes such as catastrophic landslides, volcanic debris avalanches, and outburst flows from failures of natural dams are a dominant source of sediment. The impact and extent of these large natural events are possibly amplified by human activities. Before quantitative estimates of human acceleration of erosion can be made, human-induced sediment fluxes have to be disentangled from natural benchmark denudational fluxes. To do so, an erosion acceleration factor (EF_{human}) will be determined as the ratio of the total sediment flux, E_{tot} , to the natural benchmark (or geological) denudational mass flux, E_{geol} :

$$EF_{human} = \frac{E_{tot}}{E_{geol}} \quad (2)$$

When replacing Eq. (1) in Eq. (2), a simple model for erosion regulation potential in function of human disturbance to natural vegetation is obtained:

$$EF_{human} = \frac{a_1 \times e^{-b_1 C}}{a_2 \times e^{-b_2 C_{ref}}} = k_1 \times e^{k_2(C_{ref}-C)} \quad (3)$$

where EF_{human} is the human acceleration of erosion rates, C (%) is the modern vegetation cover as a result of human disturbance, and C_{ref} (%) is the vegetation cover of an undisturbed ecosystem for a given climatic, topographic and geological setting. The parameters a_1 , and a_2 are constants that depend on the erodibility of the terrain as function of the local climate, topography and geological setting. The empirical parameters b_1 , b_2 and k_2 are constants reflecting the efficiency of the vegetation to control erosion rates. If the total erosion rates measured for undisturbed settings are representative for the natural benchmark erosion rates, then $a_1 = a_2$ and the parameter k_1 equals one.

Methods and data

The parameters of the erosion regulation model will be calibrated with field measurements from two

mountainous regions. Field observations are collected at the spatial scale of small catchments (0.1 up to 276 km²), as this allows to analyse various erosion processes acting together at the landscape scale. Field data of the human impact on mountain erosion are obtained from the combination of three independent methods: (1) in situ produced cosmogenic radionuclides to establish natural benchmark mass denudational fluxes, (2) reservoir sedimentation measurements to establish total specific sediment yields, and (3) remote sensing to characterise vegetation cover.

Recent studies have demonstrated that spatially averaged denudational fluxes derived from in situ produced cosmogenic ¹⁰Be concentrations in river sediments allow to establish a natural benchmark against which human-induced changes in sediment flux rates can be assessed (Hewawasam et al. 2003; Bierman et al. 2005; Vanacker et al. 2007). Cosmogenic nuclides are produced in situ when (secondary) cosmic rays reach the Earth's surface. For erosion studies, the most widely used cosmogenic nuclide is currently ¹⁰Be produced in quartz minerals (von Blanckenburg 2005). In the case of steady erosion, the production of cosmogenic nuclides equals the removal of nuclides at the surface by erosion. Long-term denudation rates, E_{geol} (mm year⁻¹), can then be derived from measurements of the concentration of in situ produced cosmogenic nuclides, C_{10Be} (at g⁻¹):

$$C_{10Be} = \frac{P_0}{\left(\lambda + \frac{E_{geol}}{z^*}\right)} \quad (4)$$

where P_0 (at g⁻¹ year⁻¹) is the production rate of cosmogenic nuclides at the surface in a given mineral, λ (year⁻¹) is the decay constant of the cosmogenic nuclide, and z^* is the absorption depth scale (mm). The derived erosion rates, E_{geol} , integrate over a period determined by the time it takes to erode ~0.6 m of bedrock, and typically integrate over 5–25 k year in mountain regions. Because of the long averaging time, ¹⁰Be-based erosion rates average out episodic fluctuations in sediment fluxes and reflect long term erosion rates dominated by the natural pre-anthropogenic background erosion (von Blanckenburg 2005).

All data on cosmogenic ¹⁰Be-derived denudational fluxes presented here are derived from in situ ¹⁰Be concentration measurements in quartz minerals present in river sediments. Samples were integrated by collecting ca. 4,000 g of sediment in the active part of

the stream channel, at the outlet of small catchments ranging in size from 0.1 to 276 km² (Vanacker et al. 2007, Fig. 1 herein; Bellin et al. in press, Fig. 2 herein). Large catchments containing manmade dams were avoided as they change sediment mobilization patterns. ¹⁰Be was extracted from purified quartz using standard separation methods described in von Blanckenburg et al. (1996) and (2004). Typical sample weights were c. 20–50 g pure quartz and c. 300 µg of ⁹Be carrier was added to each sample with a measured ¹⁰Be/⁹Be ratio of $0.62 \pm 0.27 \times 10^{-14}$. The ratios were normalized to the ETH in-house secondary standard S2007N with a nominal value of ¹⁰Be/⁹Be of 28.1×10^{-12} (Christl et al. 2013). The calculated ¹⁰Be concentrations with their corresponding analytical errors and the ¹⁰Be-derived catchment-wide denudation rates for both regions are listed in Appendix Tables 1 and 2.

Total specific sediment yields are derived from sedimentation rates in small reservoirs formed by checkdams. These small dams were implemented in ephemeral streams in degraded mountainous regions for sediment trapping and stream stabilisation. They typically have a storage capacity, *V*, of 10–5,000 m³, and collect surface runoff from a drainage area of 0.1–10 km². Appendix Tables 1 and 2 resume the specific sediment yields that were measured in both regions. The sediment volume, *V* (m³), accumulated behind the checkdams was calculated from field measurements of the length, width and depth of the sedimentation obtained from high-resolution laser distance meter (Leica DistoTM A8) and depth augering. We refer to Bellin et al. (2011) for a full description of the field measurements that were used in both regions. The catchment-wide total erosion rate, *E*_{tot} (mm year⁻¹), is then calculated as following:

$$E_{tot} = \frac{V}{A \times \Delta T \times TE} \times 10^{-3} \quad (5)$$

where *V* (m³) is the estimated volume of the accumulated sediment, *A* (km²) is the surface area of the drainage basin, ΔT (year) is the filling time of the checkdams, and *TE* (%) is the sediment trap efficiency of the dams. The volume of sediments that is accumulated behind the structures, *V*, is an underestimation of the total sediment volume that is mobilised in the stream channel, as part of the suspended sediment can bypass the dam structure. As no information is available on the hydraulics of the dam

structures, the empirical formula of Brown (1943) was used to get a first estimate of the trapping efficiency, *TE* (%), of the checkdams in the Betic Cordillera:

$$TE = \left(1 - \frac{1}{1 + 0.0021 \times D \times \frac{SC}{A}} \right) \times 100 \quad (6)$$

where *SC* (m³) is the storage capacity of the reservoir and *D* is an empirical parameter depending on the characteristics of the reservoir. In this study, a *D* value of 1 was used to estimate the *TE* of the checkdams in the Betic Cordillera following Verstraeten and Poesen (2000). In the tropical Andes, most of the checkdams consist of gabions reinforced with concrete, resulting in little water loss before the checkdam is actually overtopped. Considering this as well as the relatively coarse nature of the sediments transported, the trap efficiency is estimated to be 90 % during the filling time of these small constructions (Molina et al. 2008). The total error (*TE*) on the catchment-wide erosion rates estimated using the above-mentioned method typically ranges between 40 and 50 % (Sougnuez et al. 2011). This encompasses errors due to uncertainty in the estimated filling time of the checkdams, the accumulated sediment mass as well as errors related to the estimation of *TE*.

The overall vegetation cover (*C*, %) is derived for each drainage basin, and refers to the fraction of the surface that is covered by vegetation. It is estimated based on detailed land cover type maps and vertical photographs of vegetation plots. Land cover maps for the two regions are derived from very high resolution remote sensing data. In the case of the tropical Andes, aerial photographs are used for land cover mapping; whereas very high resolution satellite images (Quickbird) are used for the Spanish Betic Cordillera (Vanacker et al. 2007; Sougnuez et al. 2011). Seven land cover classes were distinguished in the tropical Andes (native forest, pine forest, eucalyptus forest, shrubland, arable land, rangeland and barren land, see Molina et al. 2008), and five land cover classes were distinguished in the Betic Cordillera (almond orchards, abandoned almond orchards, reforested areas, crop fields and shrubland/maquis area, see Sougnuez et al. 2011). For each land cover class, 10–35 vegetation plots of 1 by 1 m were located on the reference land cover map. The surface vegetation cover was assessed visually from vertical photographs of the soil surface. The vertical photographs are processed in a standard photo program

(Gimp) to differentiate automatically vegetation from bare soil, and to calculate the ratio of vegetated pixels to the total number of pixels in the photograph. For each drainage basin, the overall vegetation cover (%) is then calculated by taking the weighted average of the surface vegetation cover of all land cover types that prevail in the drainage basin, using the area of each land cover class as the weighting factor.

Study regions

Two mountainous regions with highly contrasting land use history, climate and geological setting were selected to calibrate the erosion model. The Austro Ecuatoriano is located in the Southern part of the Ecuadorian Andes. Total catchment-wide erosion rates are calculated based on sediment volumes accumulated behind 106 checkdams in 37 small catchments (0.01 up to 16 km², Molina et al. 2008). Long-term denudation rates are established for 19 catchments ranging in size from 0.01 up to 276 km². For 8 out of 19 catchments, both long-term and modern erosion rates are measured. For the location map of the study area, we refer to Fig. 1 in Vanacker et al. (2007). The area is highly susceptible to erosion due to its rough topography, erosive climate, and shallow soils developed on poorly consolidated sedimentary and metasedimentary rocks (Vanacker et al. 2007). The area is characterized by steep topography: more than 60 % of the area has slope gradients steeper than 0.3 m/m. The Austro Ecuatoriano has a typical tropical mountain climate. Average monthly air temperatures show little variation (between 15 °C in January and 14 °C in August in Cuenca, at 2,530 m a.s.l.). Rainfall regime is bimodal with two rainy seasons, registering between 600 and 1,000 mm of yearly rainfall in Cuenca (Molina et al. 2008). Remnants of undisturbed ecosystems exist where a characteristic sequence of six vegetation zones can be found along the altitudinal gradient: glacial ice (above c. 4,900 m), desert paramos (between c. 4,900 and 4,500 m), shrub and cushion paramos (between c. 4,500 and 4,000 m), grass paramos (between c. 4,000 and 3,400 m), upper montane rain forest (between c. 3,400 and 2,500 m) and montane shrub vegetation (between 3,000 and 2,000; Keating 1999). Successive periods of land clearing and abandonment resulted in strong anthropogenic disturbance to the forest

ecosystems. This was particularly important in the 1960s and 1970s when rapid socio-economic and demographic changes resulted in accelerated deforestation, agricultural colonisation and urban expansion (Wunder 1996; Vanacker et al. 2003). It is estimated that 90 % of the native forests has been converted to agricultural land (cropland and grassland) or has been replaced by secondary woody vegetation or, more recently, by exotic species (Guns and Vanacker 2013).

The Betic Cordillera is the westernmost segment of the European Alpine belt, and is characterized by a succession of mountain ranges that are mainly oriented in an E–W direction. Study sites are located in the Sierras de Los Filabres, Alhamilla and Cabrera bordering the Tabernas Desert, the Sierra de las Estancias, Sierra Torrecilla; and Sierra Almagrera. Total catchment-wide erosion rates are here estimated from the volume of sediment deposited behind checkdams in 54 catchments (0.01 up to 9 km², Bellin et al. 2011; Sougnez et al. 2011), and long-term denudation rates are obtained for 20 catchments (0.01 up to 14 km², Bellin et al. in press). 10 catchments are sampled for both modern and long-term erosion rates. The sampled catchments are distributed randomly in the Internal Zone of the Betic Cordillera, and can therefore be considered to be representative of the environmental settings in this region. The lithology consists of micaschist, quartzites, and phyllites with local outcrops of limestone and dolomite rocks. Soils are generally shallow as illustrated by the dominance of regosols and lithic leptosols. The climate is semi-arid with dry and warm summers and mild winters, a low annual rainfall with strong variability (increasing with altitude from about 300 to 650 mm). In contrast to the Austro Ecuatoriano where smallholder agriculture dominates the landscape, traditional mountain agriculture has largely been abandoned in the Spanish Betic Cordillera (MacDonald et al. 2000; Boix-Fayos et al. 2007). Agricultural land occupies less than 5 % of the surface area (Bellin et al. 2011). Land abandonment already started in the 1940s and continued at faster rates after the 1960s (Garcia-Ruiz 2010). More than 30 years after the main phase of land abandonment, the dominant vegetation type is matorral, characterized by a sclerophyllous and thorny vegetation. Tree cover is very scattered with the presence of some remnants of mesophilous taxons at higher altitudes. During the last decades, afforestation with indigenous pines (*pinus halepensis*, *pinus laricina*,

silvestris, uncinata and canariensis), Pinus radiata and Eucalyptus has been important at high altitudes and steep slopes. Southeast Spain is commonly reported as the European region that is most affected by erosion, but the role of humans in accelerating erosion processes is still subject of active debate (Wainwright and Thornes 2004).

Results and discussion

Total erosion rates as a function of vegetation cover

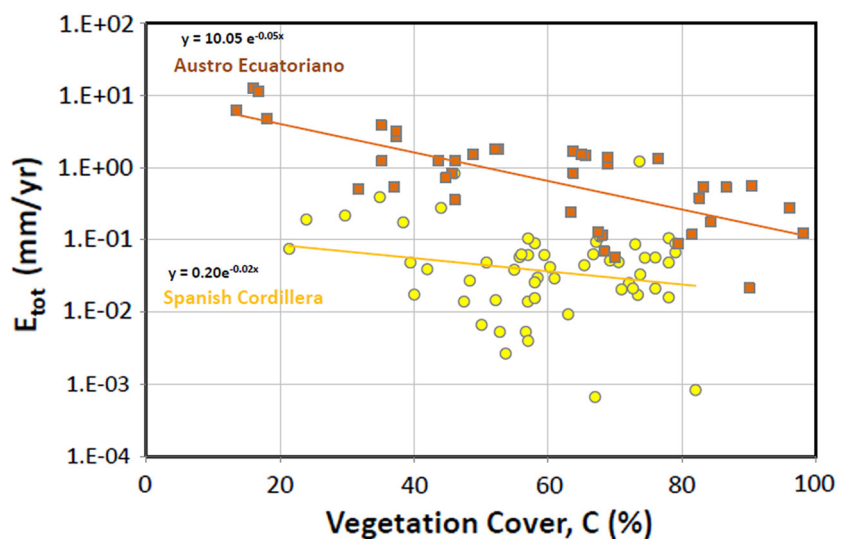
In both mountainous regions, the total erosion rates, E_{tot} , are inversely related to the overall vegetation cover, C (Fig. 2). The monotonous, nonlinear decrease of erosion rates with increasing vegetation cover is remarkably similar to the empirical relations that were derived for splash, interrill and rill erosion from experimental plot experiments (see Gyssels et al. 2005). It also confirms earlier observations by Wischmeier and Smith (1978) and Thornes (1990) that sites with very low to low vegetation cover are particularly vulnerable to erosion. Total erosion rates are systematically higher (about ten times) in the Austro Ecuatoriano compared to the Internal Zone of the Betic Cordillera. The catchment-wide erosion rates typically show a large variability in both regions. They range between 0.01 and 18.4 $\text{Mg ha}^{-1} \text{ year}^{-1}$ (with mean value of 1.5 $\text{Mg ha}^{-1} \text{ year}^{-1}$) in the Spanish

site, and between 0.26 and 151 $\text{Mg ha}^{-1} \text{ year}^{-1}$ (mean value: 21.9 $\text{Mg ha}^{-1} \text{ year}^{-1}$) in the Ecuadorian site. Although the specific sediment yields that are reported for the Spanish site are quite low, they agree with previous erosion rate studies by Puigdefabrigas et al. (1999), Boix-Fayos et al. (2007) and Romero-Diaz et al. (2007).

The systematic difference in catchment-wide erosion rates is not related to differences in the overall vegetation cover between the two regions, but is likely to be related to the more erosive setting in the Southern Ecuadorian Andes; characterised by very steep terrain, highly erodible bedrock and active tectonism (Vanacker et al. 2007). Two important observations can be made based on Fig. 2. First, the strength of the relation between erosion rates and vegetation cover varies strongly with the local environmental setting. For the Austro Ecuatoriano, the erosion data are tightly clustered along the regression line. The opposite is true for the semi-arid Internal Zone of the Betic Cordillera, where the erosion rates vary by two orders of magnitude for a given range of vegetation cover. This is likely to be linked to the extreme spatial and temporal variability of rainfall that is characteristic for this semi-arid Mediterranean climate. As most of the erosion is produced during extreme high-intensity rainfall events (Canton et al. 2011), we might expect large variation in erosion rates depending on the presence/absence of extreme rainfall events during the erosion record.

Second, our data suggest that vegetation is far more efficient for erosion and sediment control in a tropical

Fig. 2 Total erosion rates as a function of vegetation cover for the Austro Ecuatoriano (orange rectangles) and the Spanish Cordillera (yellow dots). The dependency of erosion rates to vegetation cover depends largely on the local environmental setting, where vegetation is far more efficient in controlling erosion rates in the Austro Ecuatoriano. (Color figure online)



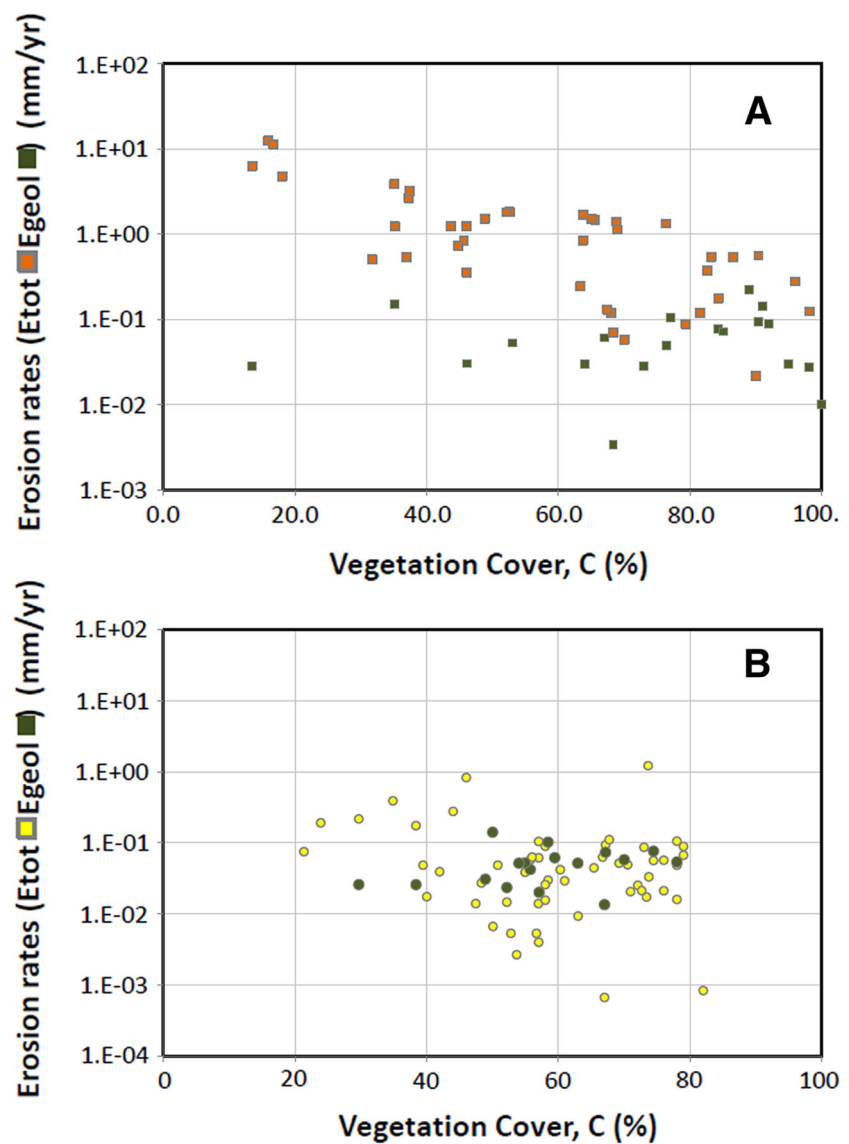
environment compared to a semi-arid setting as the slope of the regression between erosion rates and vegetation cover (parameter b in Eq. 1) equals 0.05 for the Austro Ecuatoriano and 0.02 for the semi-arid Betic Cordillera. This suggests that the effectiveness of the vegetation cover to reduce erosion rates is not constant, but depends on the local environmental setting. The protective effects of vegetation covers might be limited in Mediterranean climates characterised by torrential rainfall with intensities of more than 200 mm/24 h (De Luis et al. 2000). During such high-intensity storms, the rainfall intensity largely exceeds the soil infiltration rates (Puigdefabrigas

2005). Surface runoff generation, the main driver of soil erosion and sediment mobilisation, occurs then independent of vegetation cover.

Natural erosion benchmarks to quantify human-induced erosion

The impact of human disturbances to erosion and sediment mobilisation cannot be assessed solely based on modern erosion rates. It is necessary to compare total erosion rates, E_{tot} , with natural benchmark erosion rates, E_{geol} , to assess human-induced changes in erosion rates. Figure 3 nicely illustrates this concept.

Fig. 3 Total and natural benchmark erosion rates as a function of vegetation cover for **a** Austro Ecuatoriano and **b** Spanish Betic Cordillera. Geological erosion rates are independent of the modern vegetation cover. For a given range of vegetation cover, the difference between E_{tot} and E_{geol} is an indicator of the human acceleration of erosion



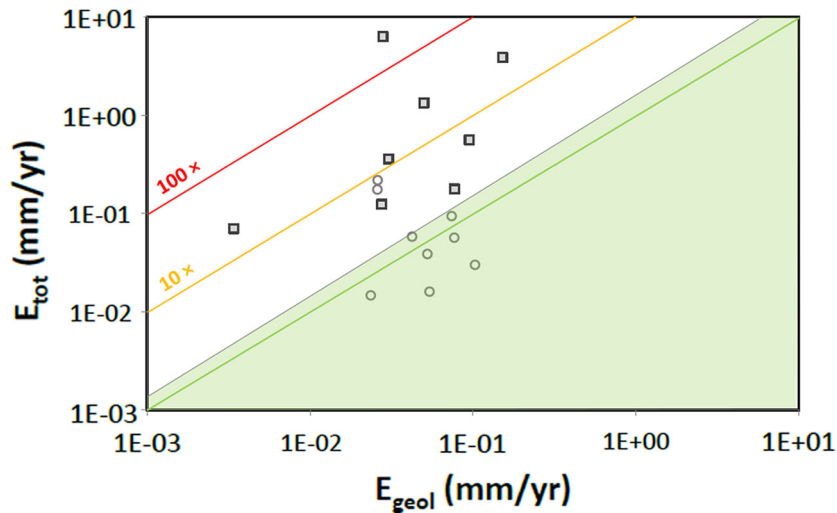


Fig. 4 Scatterplot of total erosion rates (E_{tot}) against natural benchmark erosion benchmarks (E_{geol}). The figure only shows the values for drainage basins in the Spanish Cordillera (*grey dots*) and the Austro Ecuatoriano (*grey rectangles*) where both total

erosion and long-term erosion rates were measured. The green zone corresponds to the area of the graph where total and natural benchmark erosion rates are not significantly different, given the uncertainty on the erosion values

In the semi-arid Spanish Cordillera, total catchment-wide erosion rates are not significantly different from natural, geological denudation rates. Figure 3b shows that the range of total catchment-wide erosion rates ($E_{\text{tot}} = 0.096 \pm 0.198 \text{ mm year}^{-1}$) overlaps with the geological denudation rates ($E_{\text{geol}} = 0.062 \pm 0.049 \text{ mm year}^{-1}$), although modern erosion rates are characterised by a larger variability. The opposite is true for the Austro Ecuatoriano, where modern erosion rates for disturbed sites are systematically one to two orders of magnitude higher than the benchmark erosion rates (Fig. 3a). The difference between the total erosion and the natural benchmark strongly increases with decreasing vegetation cover and, hence, increasing vegetation disturbance. For highly disturbed catchments with an overall vegetation cover below 50 %, there is a 100-fold to 1,000-fold increase in erosion rates compared to the natural benchmark erosion rates. On the other hand, weakly disturbed catchments with an overall vegetation cover above 80 % have modern erosion rates that are not significantly different from the natural benchmark erosion rates.

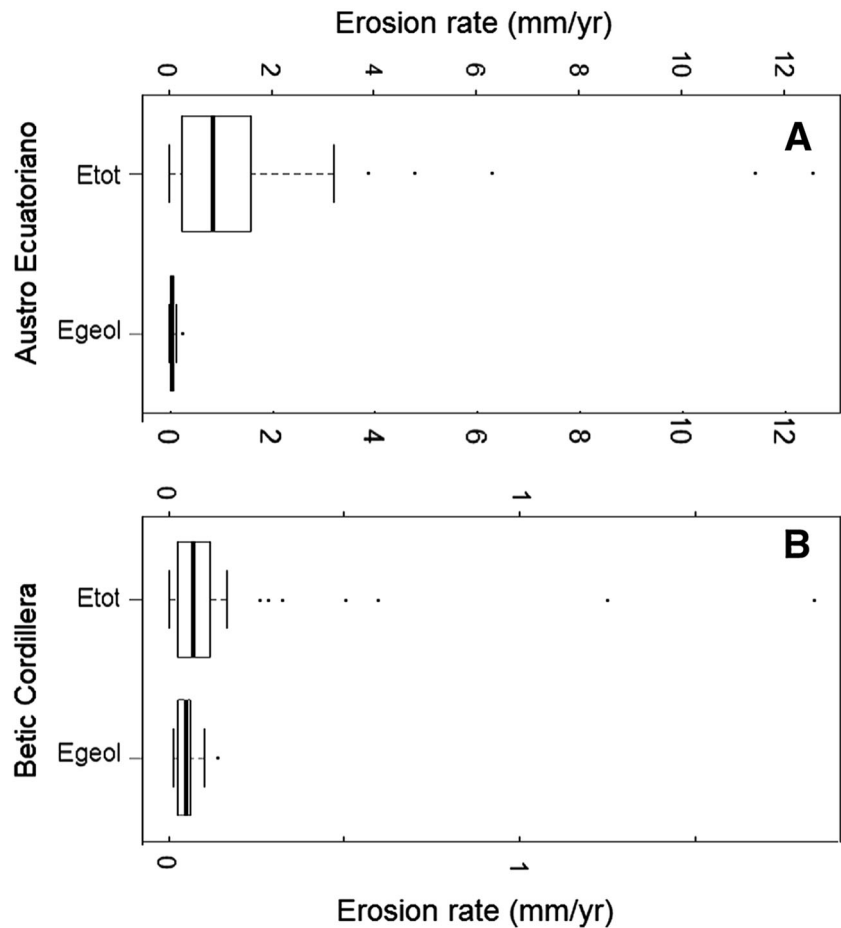
Our data show evidence that modern erosion rates are not necessarily equivalent to human-induced erosion rates, as natural erosion rates can be important in mountainous terrain. Although the Spanish Cordillera

is commonly characterized as being highly degraded as a result of past land use change (Brandt and Thornes 1996), it becomes evident that modern acceleration of erosion by human activities is generally not supported by the erosion data from the Spanish sites. When comparing total erosion with benchmark erosion rates for the same drainage basins (Fig. 4), it becomes clear that seven out of ten Spanish catchments have no significant changes in erosion due to human disturbance. Only for cultivated sites covered with rainfed orchards, human acceleration of erosion is evident. van Wesemael et al. (2006) showed very high soil redistribution rates (up to $5.5 \text{ Mg ha}^{-1} \text{ year}^{-1}$) in rainfed tree crops due to tillage and water erosion. The situation is very different for the Austro Ecuatoriano, where the share of geological erosion in the total erosion rate is minimal for most small catchments (Fig. 4).

Human acceleration of erosion as a function of vegetation cover

When comparing the magnitude–frequency distribution of modern and natural benchmark erosion rates, we observe a clear decrease in the frequency of low-magnitude events for modern erosion rates (Fig. 5). This change is most pronounced for the Austro Ecuatoriano, where the frequency of occurrence of low-magnitude

Fig. 5 Boxplot of total and natural erosion rates for for **a** Austro Ecuatoriano and **b** Spanish Betic Cordillera. Compared to natural erosion rates, the total erosion rates have a lower frequency of low-magnitude erosion rates. The shift in the frequency–magnitude distribution is most evident for the Austro Ecuatoriano



events (i.e. events with erosion rates lower than $0.025 \text{ mm year}^{-1}$) drops by about 75 %. The shift in magnitude–frequency of erosion rates is less pronounced for the Spanish site, although not negligible.

The erosion acceleration factor (EF_{human}) gives a quantitative estimate of the overall change in erosion rate. It is calculated following Eq. (2) as the ratio of the total (E_{total}) to the natural benchmark erosion rate (E_{geol}). Given the uncertainty on the erosion estimates, it can be conservatively assumed that any value of EF_{human} that is lower than 2 does not represent any real change in erosion rate. The total uncertainty on the EF_{human} values is not only related to the uncertainties on the total catchment-wide erosion and long-term denudation rates, but also to the different temporal scale over which erosion rates are integrated.

Figure 6 shows the erosion acceleration factor as a function of vegetation disturbance. Here, we estimate the vegetation disturbance by a simple proxy that

equals the difference between the current, measured vegetation cover (C) and the (hypothetical) vegetation cover of an undisturbed site for a similar climatic, topographic and geological setting (C_{ref} , %). There is a clear difference in the vegetation cover that can be expected in undisturbed sites between the two regions. For the Austro Ecuatoriano, there is no doubt that the undisturbed ecosystems have a continuous plant cover of generally 100 % (Keating 1999). There exists less information on the vegetation that would be characteristic for undisturbed sites in the Spanish Cordillera, as human occupation has strongly altered the overall vegetation composition and density (Bellin et al. in press). Based on the vegetation characterization of restored sites, we assume that the vegetation cover of undisturbed sites would approximate 75 to 80 % in this semi-arid environment. This also corresponds to the maximum vegetation cover that was measured for dense matorral (Sougnuez et al. 2011).

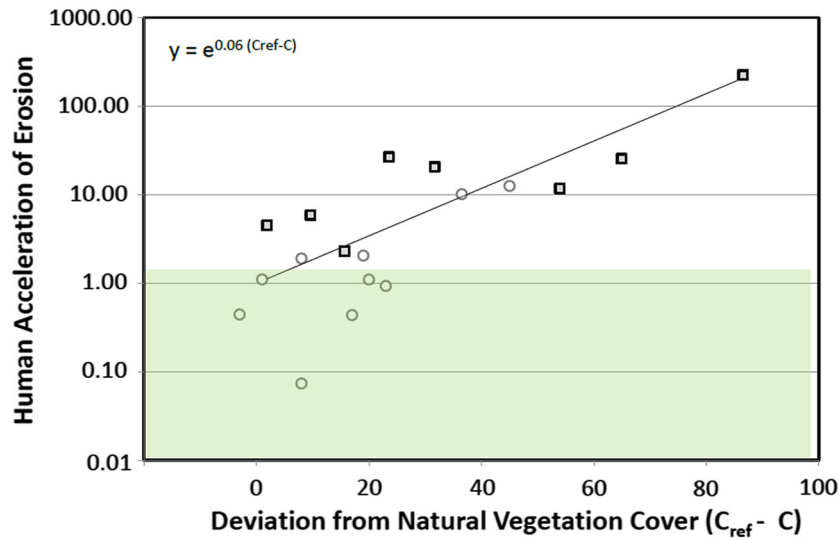


Fig. 6 Human erosion acceleration (EF_{human}) as a function of vegetation disturbance ($C_{\text{ref}}-C$) for the Austro Ecuatoriano (rectangles) and the Spanish Cordillera (dots). Although the two regions strongly differ in land use history, climatic and geological setting, the data roughly follow the same trend with

This approach allows us to calibrate the erosion regulation model presented in Eq. (3) based on the observations from two environmental settings with contrasting land use history, climatic regime, and lithological contrasts. When plotting the values of human acceleration of erosion as a function of vegetation disturbance, it can be observed that the data from the two regions roughly follow the same trend. Overall, there is a significant correlation between the human acceleration of erosion and the vegetation disturbance (Pearson correlation coefficient = 0.72, $n = 18$). When fitting a regression line through the observed data, we obtain the following equation:

$$EF_{\text{human}} = e^{0.06(C_{\text{ref}}-C)} \quad (7)$$

This empirical model allows predicting the human acceleration of erosion as a function of human-induced changes in vegetation. Without any doubt, there exists a large spread in the response to vegetation disturbances that deserves further analysis. The variation is particularly important for low vegetation disturbances. However, it is not surprising that the values of EF_{human} are lower than 1 for some sites in the Spanish Cordillera. As this region is characterized by very rare but extreme rainfall events, modern (short-

term) erosion rates are likely not to include these rare storm events during which most of the sediment mobilisation occurs (Canton et al. 2011).

an exponential increase in erosion acceleration with increasing vegetation disturbance. The area shaded in green corresponds with the area of graph where there is no clear human acceleration of erosion given the uncertainty on the erosion rates

term) erosion rates are likely not to include these rare storm events during which most of the sediment mobilisation occurs (Canton et al. 2011). The potential erosion regulation model indicates that the impact of human disturbances on erosional processes largely depends on the potential changes in vegetation cover. Hence, this suggests that the sensitivity to human-accelerated erosion would be highly ecosystem-dependent. In well-vegetated ecosystems with intrinsically a greater potential for strong vegetation disturbances (as native forests are converted to agricultural land), the human-induced erosion rate may totally outweigh the long-term benchmark erosion rates. This is less evident in sparsely vegetated ecosystems, where the potential change in vegetation cover due to human activities is limited.

Conclusion

In this paper, we developed an empirical erosion regulation model that specifically accounts for the complex mixture of natural and human-induced erosion processes occurring in mountainous terrain. The erosion model predicts human acceleration of erosion as the ratio of the total erosion to the natural benchmark

erosion rate. The model was calibrated with modern and natural erosion measurements from two mountainous regions with highly contrasting land cover, climatic and geological setting: the Austro Ecuatoriano and the semi-arid Spanish Betic Cordillera. Although more data are needed from contrasting environmental settings to further test the model, the following three conclusions can be drawn when pooling the erosion data from the two mountainous sites:

First, modern erosion rates are related to vegetation cover. With decreasing vegetation cover, there is an exponential increase in total erosion rates. However, the direction and strength of this relationship strongly depend on local environmental settings. The efficiency of vegetation to control erosion rates is highest for the Austro Ecuatoriano, where the potential human disturbance to vegetation cover is most pronounced.

Second, our data show that the impact of human disturbances to erosion cannot be assessed solely based on modern erosion rates, as natural erosion rates are important in mountainous terrain. This is particularly the case in the Internal Zone of the Spanish Cordillera, where modern erosion rates are not significantly different from natural, benchmark erosion rates although they display a larger variability. This also questions the direct use of modern erosion rates as indicators of human disturbance to erosion regulation.

Third, our data suggest that the human acceleration of erosion defined as the ratio of total to natural erosion rates is an exponential function of vegetation disturbance. Human-induced changes in erosion rate are likely to depend on the magnitude of vegetation disturbance. Our empirical data from two contrasting regions suggest that the sensitivity to human-accelerated erosion might be ecosystem-dependent, where well-vegetated ecosystems are more sensitive due to their greater exposure to strong vegetation disturbances. Therefore, it suggests that the potential for erosion regulation is larger in well-vegetated ecosystems compared to sparsely vegetated systems.

Acknowledgments We thank M. Bravin, R. Ortega and N. Sougnez for their help during the sampling campaign. This work received financial support from the Fonds de la Recherche Scientifique (FRS) and the Communauté Française. A. Molina was funded by the Alexander von Humboldt Foundation. R. Ortega was supported by a Marie Curie postdoctoral fellowship PIEF-Ga-2009-23064 (Sedimed). The sampling in Ecuador was facilitated through an inter-university research project (PIC) funded by CIUF-CUD (Commission Universitaire pour le Développement) at the University of Cuenca (Ecuador).

Appendix

Table 1 Main characteristics of the sampled catchments in the Austro Ecuatoriano

Sample	Latitude (DD)	Longitude (DD)	Basin area (km ²)	Fractional vegetation cover (<i>f</i>)	¹⁰ Be denudation rate (mm/year)	Total erosion rate (mm/year)
BQ	−2.894	−78.893	186.3	0.53	0.053 ± 0.004	
CJ	−2.917	−78.870	19.5	0.90	0.095 ± 0.011	0.56
DE2	−2.767	−78.920	39.1	0.77	0.105 ± 0.009	
JA2 ¹	−2.873	−78.883	276.0	0.76	0.052 ± 0.005	1.33
JA2 ^{2–3–4}					0.048 ± 0.004	
MA1	−3.040	−78.948	0.1	0.14	0.028 ± 0.003	6.32
MAR	−3.040	−78.949	49.8	0.64	0.030 ± 0.002	
NA1	−2.699	−78.268	57.1	0.91	0.142 ± 0.018	
NA4	−2.663	−78.901	4.9	0.89	0.222 ± 0.033	
QU	−3.021	−78.915	16.7	0.84	0.077 ± 0.008	0.18
RGST	−2.959	−78.895	20.2	0.73	0.028 ± 0.002	
RG ^{1–2}	−2.955	−78.892	0.9	0.98	0.025 ± 0.002	0.12
RG ^{3–4}					0.028 ± 0.002	

Table 1 continued

Sample	Latitude (DD)	Longitude (DD)	Basin area (km ²)	Fractional vegetation cover (<i>f</i>)	¹⁰ Be denudation rate (mm/year)	Total erosion rate (mm/year)
RG2	−2.909	−78.900	29.2	0.67	0.061 ± 0.006	
RGD ¹	−2.936	−78.796	2.2	0.46	0.027 ± 0.002	0.36
RGD ²					0.031 ± 0.003	
RGD ^{3–4}					0.033 ± 0.003	
SA	−2.952	−78.923	0.5	0.35	0.152 ± 0.019	3.88
SF ^{1–2}	−2.891	−78.771	84.0	0.85	0.061 ± 0.006	
SF ³					0.079 ± 0.007	
SF ⁴					0.077 ± 0.008	
SI1	−3.158	−78.815	0.6	0.38	0.010 ± 0.001	
SI2	−3.142	−78.810	18.3	0.29	0.030 ± 0.003	
SI3	−3.137	−78.811	49.2	0.18	0.088 ± 0.011	
SI5	−2.988	−78.809	6.0	0.68	0.003 ± 0.001	0.07
VAL1	−2.873	−78.883	<0.1	0.53		1.62
VAL3	−2.873	−78.883	<0.1	0.52		1.61
BEL	−2.869	−78.875	9.4	0.82		0.11
VEGA	−2.870	−78.876	0.3	0.18		4.27
SIP	−3.003	−78.812	0.1	0.37		2.38
CAL	−2.805	−78.909	1.5	0.16		11.19
MES2	−2.800	−78.898	<0.1	0.49		1.35
MES1	−2.800	−78.898	<0.1	0.35		1.10
AU	−2.816	−78.879	<0.1	0.17		10.15
LLAY	−2.870	−78.839	<0.1	0.90		0.02
PES	−2.926	−78.794	7.1	0.68		0.11
UZ1	−2.933	−78.796	0.6	0.32		0.45
AGU	−2.944	−78.794	16.1	0.67		0.12
ARG	−3.003	−78.853	1.5	0.79		0.08
DUN	−2.946	−78.815	0.2	0.69		1.00
LLAN	−3.007	−78.929	4.6	0.70		0.05
QUI1	−3.029	−78.915	7.3	0.96		0.25
QUI2	−3.030	−78.914	4.3	0.83		0.48
QUI3	−3.023	−78.909	1.3	0.63		0.22
SALJ	−2.956	−78.928	0.6	0.37		0.48
ANT	−2.941	−78.927	0.3	0.37		2.86
CHO	−2.951	−78.930	0.2	0.64		1.52
AGS	−2.716	−78.893	0.3	0.44		1.10
SJUNB	−2.714	−78.892	2.1	0.64		0.76
TURU1	−2.715	−78.893	2.9	0.69		1.25
TURU2	−2.714	−78.891	3.3	0.66		1.32
TURU3	−2.714	−78.890	5.5	0.65		1.35
SALB1	−2.795	−78.931	1.3	0.46		0.75

Table 1 continued

Sample	Latitude (DD)	Longitude (DD)	Basin area (km ²)	Fractional vegetation cover (<i>f</i>)	¹⁰ Be denudation rate (mm/year)	Total erosion rate (mm/year)
SALB2	−2.798	−78.929	1.9	0.46		1.11
NEG	−2.806	−78.920	3.4	0.45		0.64

Catchment-wide erosion rates are calculated based on sediment volumes accumulated behind 106 checkdams for 37 small catchments (Molina et al. 2008), and on bathymetric data for the JA2 catchment only. Long-term denudation rates are established based on ¹⁰Be concentrations in river sediments of 19 catchments (Vanacker et al. 2007)

Quartz was extracted from the 0.25–2.5 mm grain size fraction of the alluvial material. For five samples, we analysed the effect of grain size (¹0.25–0.85 mm. ²0.85–1.25 mm. ³1.25–2.0 mm. ⁴2.0–2.5 mm) on the ¹⁰Be concentration. No significant difference in ¹⁰Be concentration was observed between grain size fractions, and the remaining ¹⁰Be analyses were realized on the 0.250–1.250 mm fraction. The ¹⁰Be concentrations that were measured prior to April 2010 were renormalized relative to the new half-life and AMS standardization by reducing the old ¹⁰Be concentrations by a factor of 1.096 as suggested by Christl et al. (2013)

Table 2 Main characteristics of the sampled catchments in the Spanish Betic Cordillera

Sample	Latitude (DD)	Longitude (DD)	Basin area (km ²)	Fractional vegetation cover (<i>f</i>)	¹⁰ Be denudation rate (mm/year)	Total erosion rate (mm/year)
204	37.020	−2.300	1.49	0.71		0.049
200	26.340	−2.390	0.12	0.67		0.063
203	37.010	−2.370	1.51	0.72		0.025
202a	37.000	−2.380	2.85	0.73		0.017
70	37.580	−2.210	0.04	0.35		0.393
NEWESTAN1	37.588	−2.182	0.21	0.38	0.026 ± 0.003	0.175
176	37.600	−2.080	0.70	0.60		0.042
153b	37.590	−2.100	0.28	0.69		0.052
154b	37.590	−2.090	0.60	0.74		0.033
180a	37.600	−2.050	0.46	0.42		0.039
NEWESTAN3	37.592	−2.054	0.21	0.30	0.026 ± 0.003	0.218
69	37.580	−2.190	0.40	0.39		0.049
18f	37.450	−2.420	0.50	0.48		0.027
163	37.590	−2.050	0.17	0.21		0.075
178	37.580	−2.140	0.11	0.24		0.192
16a	37.240	−2.390	9.11	0.61		0.029
31b	37.300	−2.590	3.07	0.47		0.014
NEWESTAN2	37.506	−2.216	0.70	0.74	0.077 ± 0.009	0.057
42	37.260	−2.440	3.0	0.50		0.007
FILEST1	37.328	−2.358	0.93	0.67	0.074 ± 0.008	0.094
NOFIL1	37.337	−2.622	0.46	0.58	0.103 ± 0.012	0.030
11a	37.340	−2.680	0.95	0.57		0.014
NOFIL2	37.317	−2.599	1.91	0.56	0.042 ± 0.004	0.058
16b	37.260	−2.380	5.12	0.65		0.045
56	37.320	−2.540	3.06	0.53		0.005
15a	37.310	−2.630	0.88	0.59		0.062
NOFIL4	37.308	−2.649	1.69	0.52	0.024 ± 0.002	0.015
NOFIL3	37.259	−2.449	7.77	0.55	0.052 ± 0.006	0.039

Table 2 continued

Sample	Latitude (DD)	Longitude (DD)	Basin area (km ²)	Fractional vegetation cover (<i>f</i>)	¹⁰ Be denudation rate (mm/year)	Total erosion rate (mm/year)
1	37.140	−2.520	0.71	0.57		0.005
28	37.150	−2.510	1.42	0.63		0.009
4a	37.160	−2.650	5.04	0.54		0.003
27	37.190	−2.700	5.42	0.51		0.049
3a	37.190	−2.580	0.87	0.73		0.021
9e	37.240	−2.790	2.60	0.71		0.021
9d	37.230	−2.800	4.43	0.68		0.111
9c	37.230	−2.810	0.12	0.74		1.226
CAR1	37.831	−1.337	3.09	0.58		0.016
CAR2	37.832	−1.337	3.11	0.58		0.026
CAR3	37.831	−1.340	0.16	0.44		0.278
CAR4	37.804	−1.312	0.94	0.58		0.090
CAR5	37.800	−1.313	0.17	0.57		0.062
CAR6	37.795	−1.314	0.13	0.57		0.105
CAR7	37.798	−1.313	0.59	0.57		0.004
CAR8	37.797	−1.313	0.02	0.46		0.833
TOR1	37.651	−1.826	0.14	0.73		0.087
TOR16R	37.648	−1.797	0.13	0.82		0.001
TOR5	37.652	−1.795	1.70	0.67	0.014 ± 0.002	0.001
TOR6	37.643	−1.793	0.19	0.78	0.054 ± 0.006	0.016
TOR28	37.655	−1.746	0.23	0.78		0.106
TOR29	37.656	−1.747	0.14	0.79		0.067
TOR14102_1	37.666	−1.805	0.06	0.40		0.018
TOR140101_1	37.666	−1.807	0.05	0.56		0.063
TOR140102_2	37.667	−1.806	0.07	0.76		0.057
TOR140102_3	37.667	−1.808	0.22	0.76		0.021
EST01	37.552	−1.793	0.14	0.57	0.020 ± 0.002	
EST02	37.576	−2.114	0.05	0.54	0.020 ± 0.002	
ALH01	37.028	2.176	14.40	0.59	0.060 ± 0.008	
ALM01	37.325	−1.754	0.70	0.70	0.058 ± 0.006	
CAB01	37.095	−1.835	0.25	0.50	0.142 ± 0.018	
CAB02	37.065	−1.895	7.72	0.54	0.104 ± 0.014	
CAB03	37.053	−1.939	1.99	0.62	0.246 ± 0.031	
FIL01	37.178	−2.034	8.63	0.54	0.052 ± 0.006	
FIL02	37.172	−2.040	3.34	0.63	0.052 ± 0.006	
FIL03	37.230	−2.106	0.26	0.49	0.031 ± 0.003	

Catchment-wide erosion rates are calculated based on sediment volumes accumulated behind checkdams in 54 small catchments (Bellin et al. 2011; Sougnez et al. 2011). Long-term denudation rates are established based on ¹⁰Be concentrations in river sediments of 20 catchments (Bellin et al. in press)

References

- Arnold JG, Moriasi DN, Gassman PW, Abbaspour KC, White MJ, Srinivasan R, Santhi C, Harmel RD, van Griensven A, Van Liew MW, Kannan N, Jha MK (2012) SWAT: model use, calibration, and validation. *Trans ASABE* 55:1494–1508
- Bellin N, Vanacker V, van Wesemael B, Sole-Benet A, Bakker MM (2011) Natural and anthropogenic controls on soil erosion in the Internal Betic Cordillera (southeast Spain). *Catena* 87:190–200
- Bellin N, Vanacker V, De Baets S (in press) Anthropogenic and climatic impact on Holocene sediment dynamics in SE Spain: a review. *Quat Int*. doi:10.1015/j.quaint.2013.03.015
- Bellin N, Vanacker V, Kubik PW (in press) Constraining denudation rates along a gradient of slow tectonic uplift in the Betic Cordillera, southeast Spain. *Earth Planet Sci Lett*
- Bierman PR, Reuter JM, Pavich M, Gellis AC, Caffee MW, Larsen J (2005) Using cosmogenic nuclides to contrast rates of erosion and sediment yield in a semi-arid, arroyo-dominated landscape, Rio Puerco Basin, New Mexico. *Earth Surf Proc Land* 30:935–953
- Boix-Fayos C, Barberá GG, López-Bermúdez F, Castillo VM (2007) Effects of checkdams, reforestation and land-use changes on river channel morphology: case study of the Rogativa catchment (Murcia, Spain). *Geomorphology* 91:103–123
- Brandt CJ, Thorne JB (1996) Mediterranean desertification and land use. Wiley, Chichester
- Brown C (1943) Discussion of sedimentation in reservoirs by J. Witzig. *Proc ASCE* 69:1493–1500
- Canton Y, Solé-Benet A, de Vente J, Boix-Fayos C, Calvo-Cases A, Asensio C, Puigdefábrigas J (2011) A review of runoff generation and soil erosion across scales in semiarid south-eastern Spain. *J Arid Environ* 75:1254–1261
- Christl M, Vockenhuber C, Kubik PW, Wacker L, Lachner J, Alfimov V, Synal HA (2013) The ETH Zurich AMS facilities: performance parameters and reference materials. *Nucl Instrum Methods Phys Res Sect B* 294:29–38
- Corenblit D, Steiger J (2009) Vegetation as a major conductor of geomorphic changes on the Earth surface: toward a Darwinian geomorphology. *Earth Surf Proc Land* 34:891–896
- De Luis M, Raventos H, Gonzalez-Hidalgo JC, Sanchez JR, Cortina J (2000) Spatial analysis of rainfall trends in the region of Valencia (East Spain). *Int J Climatol* 20:1451–1469
- Dietrich WE, Perron TJ (2006) The search for a topographic signature of life. *Nature* 439:411–418
- Fohrer N, Haverkamp S, Frede HG (2005) Assessment of the effects of land use patterns on hydrologic landscape functions: development of sustainable land use concepts for low mountain range areas. *Hydrol Process* 19:659–672
- Foley JA, DeFries R, Asner GP, Barford C, Bonan G, Carpenter SR, Chapin FS, Coe MT, Daily GC, Gibbs HK, Helkowski JH, Holloway T, Howard EA, Kucharik CJ, Monfreda C, Patz JA, Prentice IC, Namankutty N, Snyder PK (2005) Global consequences of land use. *Science* 22:570–574
- Food and Agricultural Organisation of the United Nations (2011) Why invest in sustainable mountain development?. FAO, Rome
- Garcia-Ruiz JM (2010) The effects of land uses on soil erosion in Spain: a review. *Catena* 81:1–11
- Garcia-Ruiz JM, Lasanta T, Ruiz-Flano P, Ortigosa L, White S, Gonzalez C, Marti C (1996) Land use changes and sustainable development in mountain areas: a case study in the Spanish Pyrenees. *Landscape Ecol* 11:267–277
- Guns M, Vanacker V (2013) Forest cover change trajectories and their impact on landslide occurrence in the Tropical Andes. *Environ Earth Sci*. doi:10.1007/s12665-013-2352-9
- Gyssels G, Poesen J, Bochet E, Li Y (2005) Impact of plant roots on the resistance of soil to erosion by water: a review. *Prog Phys Geog* 29:189–217
- Hewawasam T, von Blanckenburg F, Schaller M, Kubik PW (2003) Increase of human over natural erosion rates in tropical highlands constrained by cosmogenic nuclides. *Geology* 31:597–600
- Huber U, Bugmann H, Reasoner M (2005) Global change and mountain regions. An overview of current knowledge. *Advances in global change research*. Springer, Dordrecht
- Jandl R, Borsdorf A, van Miegroet H, Lackner R, Psenner R (2009) Global change and sustainable development in mountain regions. *Alpine space—man and environment*, vol 7. Innsbruck University Press, Innsbruck
- Jha S, Bawa KS (2006) Population growth, human development, and deforestation in biodiversity hotspots. *Conserv Biol* 20:906–912
- Keating PL (1999) Changes in paramo vegetation along an elevational gradient in southern Ecuador. *J Torrey Bot Soc* 126:159–175
- Lambin EF, Meyfroidt P (2010) Land use transitions: socio-ecological feedback versus socio-economic change. *Land Use Policy* 27:108–118
- Löffler J, Anschlag K, Baker B, Finch OD, Diekkrüger B, Wundram D, Schröder B, Pape R, Lundberg A (2011) Mountain ecosystem response to global change. *Erdkunde* 65:189–213
- MacDonald D, Crabtree JR, Wiesinger G, Dax T, Stamou N, Fleury P, Gutierrez Lazpita J, Gibon A (2000) Agricultural abandonment in mountain areas of Europe: environmental consequences and policy response. *J Environ Manag* 59:47–69
- Millennium Ecosystem Assessment (2005) *Ecosystems and human well-being: current state and trends*. Island Press, Washington, DC
- Molina A, Govers G, Poesen J, Van Hemelryck H, De Bièvre B, Vanacker V (2008) Environmental factors controlling spatial variation in sediment yield in a central Andean mountain area. *Geomorphology* 98:176–186
- Pauchard A, Kueffer C, Dietz H, Daehler CC, Alexander J, Edwards PJ, Arévalo JR, Cavieres LA, Guisan A, Haider S, Jakobs G, McDougall K, Millar CI, Naylor BJ, Parks CG, Rew LJ, Seipel T (2009) Ain't no mountain high enough: plant invasions reaching new elevations. *Front Ecol Environ* 7:479–486
- Puigdefábrigas J (2005) The role of vegetation patterns in structuring runoff and sediment fluxes in drylands. *Earth Surf Proc Land* 30:133–147
- Puigdefábrigas J, Solé-Benet A, Gutierrez L, del Barrio G, Boer M (1999) Scales and processes of water and sediment redistribution in drylands: results from the Rambla Honda field site in Southeast Spain. *Earth Sci Rev* 48:39–70

- Reinhardt L, Jerolmack D, Cardinale BJ, Vanacker V, Wright J (2010) Dynamic interactions of life and its landscape: feedbacks at the interface of geomorphology and ecology. *Earth Surf Proc Land* 35:78–101
- Renard KG, Foster GR, Weesies GA, McCooln DK, Yoder DC (1998) Predicting soil erosion by water: a guide to conservation planning with Revised Universal Soil Loss Equation (RUSLE). US Department of Agriculture, Agricultural Handbook No 703
- Romero-Diaz A, Alonso-Sarria F, Martinez-Lloris M (2007) Erosion rates obtained from checkdam sedimentation (SE Spain). A multi-method comparison. *Catena* 71:172–178
- Schröter D, Cramer W, Leemans R, Prentice C, Araujo MB, Arnell NW, Bondeau A, Bugmann H, Carter TR, Gracia CA, de la Vega-Leinert AC, Erhard M, Ewert F, Glendinning M, House JI, Kankaanpää S, Klein RJT, Lavorel S, Lindner M, Metzger MJ, Meyer J, Mitchell TD, Reginster I, Rounsevell M, Sabaté S, Sitch S, Smith B, Smith J, Smith P, Sykes MT, Thonicke K, Thuiller W, Tuck G, Zaehle S, Zierl B (2005) Ecosystem service supply and vulnerability to global change in europe. *Science* 310:1333–1337
- Sidle RC, Ochiai H (2006) Landslides: processes, prediction, and land use. Water resource monograph 18. American Geophysics Union, Washington, DC
- Sougnéz N, van Wesemael B, Vanacker V (2011) Low erosion rates for steep, sparsely vegetated catchments in southeast Spain. *Catena* 84:1–11
- Stehr A, Aguayo M, Parra O, Romero F, Alcayaga H (2010) Modelling the hydrologic response of a mesoscale Andean watershed to changes in land use patterns for environmental planning. *Hydrol Earth Syst Sci* 14:1963–1977
- Thornes JB (1990) Vegetation and erosion: processes and environments. Wiley, Chichester
- van Wesemael B, Rambaud X, Poesen J, Muligan M, Cammeraat E, Stevens A (2006) Spatial patterns of land degradation and their impacts on the water balance of rainfed treecrops: a case study in South East Spain. *Geoderma* 133:43–56
- Vanacker V, Govers G, Barros S, Poesen J, Deckers J (2003) The effect of short-term socio-economic and demographic change on land use dynamics and its corresponding geomorphic response with relation to water erosion in a tropical mountainous catchment, Ecuador. *Landscape Ecol* 18:1–15
- Vanacker V, von Blanckenburg F, Govers G, Molina A, Poesen J, Deckers J, Kubik PW (2007) Restoring dense vegetation can slow mountain erosion to near natural benchmark levels. *Geology* 35:303–306
- Verstraeten G, Poesen J (2000) Estimating trap efficiency of small reservoirs and ponds: methods and implications for the assessment of sediment yield. *Prog Phys Geog* 24:219–251
- Vigerstol KL, Aukema JE (2011) A comparison of tools for modeling freshwater ecosystem services. *J Environ Manag* 92:2403–2409
- Viles HA, Naylor LA, Carter NE, Chaput D (2008) Biogeomorphological disturbance regimes: progress in linking ecological and geomorphological systems. *Earth Surf Proc Land* 33:1419–1435
- Viviroli D, Dürr HH, Messerli B, Meybeck M, Weingartner R (2007) Mountains of the world, water towers for humanity: typology, mapping and global significance. *Water Resour Res* 43:W07447
- von Blanckenburg F (2005) The control mechanisms of erosion and weathering at basin scale from cosmogenic nuclides in river sediment. *Earth Planet Sci Lett* 237:462–479
- von Blanckenburg F, Belshaw N, O’Nions R (1996) Separation of ^9Be and cosmogenic ^{10}Be from environmental materials and SIMS isotope dilution analysis. *Chem Geol* 129:93–99
- von Blanckenburg F, Hewawasam T, Kubik PW (2004) Cosmogenic nuclide evidence for low weathering and denudation in the wet, tropical highlands of Sri Lanka. *J Geophys Res* 109:F3
- Wainwright J, Thornes JB (2004) Environmental issues in the mediterranean: process and perspectives from the past to the present. Routledge, London
- Wischmeier WH, Smith DD (1978). Predicting rainfall erosion losses: a guide to conservation planning. Agriculture Handbook No. 537. USDA/Science and Education Administration, US. Govt. Printing Office, Washington, DC
- Wunder S (1996) Deforestation and the uses of wood in the Ecuadorian Andes. *Mountain Res Dev* 16:367–382